

Nanocrystalline Aluminum Truss Cores for Lightweight Sandwich Structures

TOBIAS A. SCHAEGLER^{1,3}, LISA J. CHAN,² ERIC C. CLOUGH,¹
MORGAN A. STILKE,¹ JACOB M. HUNDLEY,¹
and LAWRENCE J. MASUR²

1.—HRL Laboratories, LLC, Malibu, CA, USA. 2.—Xtalic Corporation, Marlborough, MA, USA.
3.—e-mail: taschaedler@hrl.com

Substitution of conventional honeycomb composite sandwich structures with lighter alternatives has the potential to reduce the mass of future vehicles. Here we demonstrate nanocrystalline aluminum-manganese truss cores that achieve 2–4 times higher strength than aluminum alloy 5056 honeycombs of the same density. The scalable fabrication approach starts with additive manufacturing of polymer templates, followed by electrodeposition of nanocrystalline Al-Mn alloy, removal of the polymer, and facesheet integration. This facilitates curved and net-shaped sandwich structures, as well as co-curing of the facesheets, which eliminates the need for extra adhesive. The nanocrystalline Al-Mn alloy thin-film material exhibits high strength and ductility and can be converted into a three-dimensional hollow truss structure with this approach. Ultra-lightweight sandwich structures are of interest for a range of applications in aerospace, such as fairings, wings, and flaps, as well as for the automotive and sports industries.

INTRODUCTION

Sandwich structures are unique enablers of lightweight design, as they offer an exceptional combination of low density and high bending rigidity. Sandwich panels are created by attaching thin, stiff facesheets to the top and bottom surfaces of a relatively thick, lightweight core. The thickness of the core serves to separate the facesheets, thus providing the sandwich construction with high area moment of inertia, while the low density of the core allows this increased area moment of inertia to be realized for minimal mass increase. Lightweight sandwich structures are widespread in aerospace applications (e.g., winglets, flaps, rudders, and rotor blades) but are also used in many other industries. State-of-the-art sandwich panels use carbon-fiber-reinforced polymer (CFRP) composite or aluminum alloy facesheets with honeycomb or foam cores. Typical honeycomb cores are made from aluminum alloys, meta-aramid fiber paper (Nomex[®]), or glass-fiber-reinforced polymer. Closed-cell polymer foams are alternatives to honeycomb, albeit with generally lower structural performance due to their stochastic cellular architecture.¹

More recently, advanced core materials have been studied, among which the most compelling are tetrahedral and pyramidal truss structures.^{2,3} Hollow truss structures, when designed to suppress buckling, offer an opportunity for improved compressive and shear strengths versus honeycombs.^{4–6} Hollow truss structures are preferably fabricated by coating a polymer template of the truss structure, which is subsequently removed.⁷ This approach converts a two-dimensional (2D) thin film or coating into a three-dimensional (3D) cellular material, thereby redefining the applications of a range of thin film/coating materials.⁸ Thin film/coating materials with high strength and low density are sought to optimize the mechanical properties of the truss structure. Recently, an electrodepositable nanocrystalline aluminum-manganese alloy that exhibits unprecedented specific strength has been developed.⁹ In this study, we combine this high-strength nanocrystalline aluminum alloy with optimized truss architectures, resulting in sandwich cores with exceptional performance.

BACKGROUND

This study was conducted as part of the program on “Ultra-lightweight Core Materials for Efficient Load-Bearing Composite Sandwich Structures” funded by the National Aeronautics and Space Administration (NASA)’s Game Changing Development Program within the Space Technology Mission Directorate. The target application of this program was a fairing of the upper stage of NASA’s Space Launch System, which dictated a core thickness of 25.4 mm (1 in.) and a core density of 48 kg/m³. The state of the art for such fairings are lightweight sandwich structures of carbon-fiber-reinforced polymer (CFRP) facesheets bonded to a honeycomb core made of high-strength aluminum alloy 5056. Aluminum alloys offer excellent specific strength due to their low density. Xtallic Corporation has developed a nanocrystalline aluminum-manganese alloy that achieves yield strength over 1300 MPa,⁹ substantially higher than conventional wrought aluminum alloys; For example, Al 5056-H38 has yield strength of 345 MPa. While alloys with higher specific strength exist, they are typically difficult to roll into thin sheets and process into honeycombs due to their low ductility. Xtallic’s nanocrystalline aluminum-manganese alloy can be electrodeposited, which circumvents issues with formability and bodes well for fabrication of ultralight hollow truss cores. Grain sizes in the range of 10–100 nm are thermodynamically stabilized with addition of Mn, which preferentially segregates at grain boundaries and inhibits grain growth.¹⁰ More technical background on the nano Al-Mn material and processing method is provided in Ref. ¹¹.

Figure 1 compares the specific strength of relevant commercially available alloys as provided by Granta’s CES Selector,¹² from which it is evident that the performance of the nanocrystalline aluminum-manganese alloy is unrivaled. Even though advanced high-strength steels with yield strength exceeding 1800 MPa are being developed, their roughly three times higher density not only limits their specific strength, but also restricts their specific bending stiffness and bending strength. Since the bending stiffness K_{bend} and bending strength S_{bend} scale as follows according to Euler beam theory:¹³

$$K_{\text{bend}} \sim \frac{\sqrt{E}}{\rho}, \quad (1)$$

$$S_{\text{bend}} \sim \frac{\sqrt{\sigma_y}}{\rho}, \quad (2)$$

the density of a material is more important than its modulus or strength for improving bending and buckling resistance. The lower density of aluminum allows for designs with higher specific bending stiffness and specific bending strength, enabling improved bending and buckling resistance for ultra-

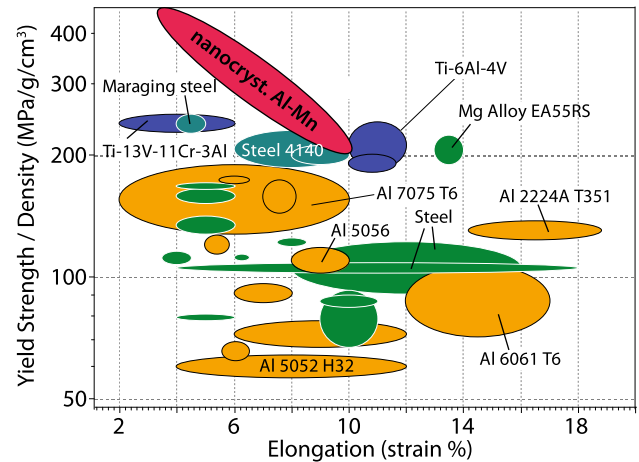


Fig. 1. Comparison of specific strength and ductility of nanocrystalline aluminum-manganese alloy with a selection of conventional alloys.

lightweight structures. This relationship can be imagined by comparing an aluminum and steel strut with the same mass and similar specific strength and modulus. In this case, the aluminum strut can have three times the cross-sectional area due to its lower intrinsic density, resulting in considerably improved bending and buckling resistance.

FABRICATION PROCESS

Core Design

For most sandwich structures as well as for NASA’s target application, transverse shear strength is the most critical mechanical property for the sandwich core. In many cases, the loading is directional, so that high shear strength in one direction is required, while the shear strengths in the orthogonal directions are of less importance. Accordingly, a hollow truss core was designed using finite element analysis following the approach described by Clough et al.⁴ A truss inclination angle α of 45° and an anisotropic unit cell with angle $\beta = 30^\circ$ were chosen to maximize the shear strength in one direction (Fig. 2). The required core thickness H of 25.4 mm (1 in.) necessitated a truss member length of 36 mm, since truss structures consisting of multiple unit cells stacked on top of each other result in lower strength than single cell layers due to the deleterious effects of nodal stress concentrations and nodal rotations.^{7,14} The nodes were designed to increase the area of contact with the facesheets and adhesive and to mitigate stress concentrations, while maintaining a fully interconnected and freestanding structure.⁴ The truss diameter D and wall thickness t were optimized for shear strength in one direction by selecting geometric parameters that mitigate local shell and global strut buckling failure modes, with the core density constrained to a value of 24 kg/m³. The finite element

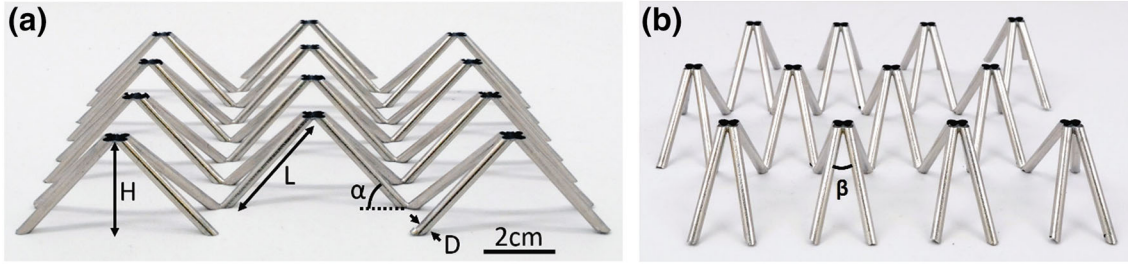


Fig. 2. Hollow aluminum truss cores with optimized anisotropic architecture, shown: (a) perpendicular to and (b) along shear direction.

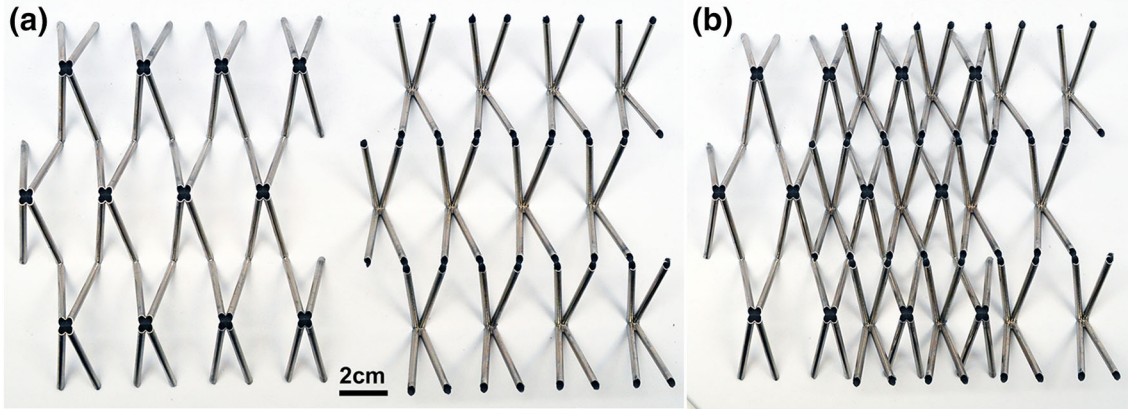


Fig. 3. Hollow aluminum truss cores: (a) from top and bottom, and (b) interlaced to increase strength and enable seamless tiling.

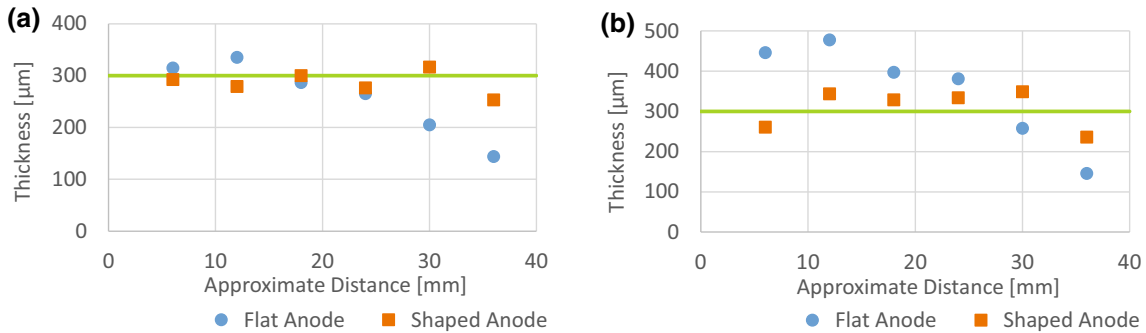


Fig. 4. Comparison of flat and shaped anode: (a) average plating thickness and (b) coating thickness underneath node as measured along the struts.

simulations suggested that a structure with strut diameter of 3.2 mm and plating thickness of 300 μm would be optimal for a hollow nanocrystalline aluminum core with the given constraints. The cores were designed so that they could be interlaced to double the density and enable seamless tiling to cover larger areas (Fig. 3).

Polymer Template Fabrication

Polymer truss structures were used as low-cost templates to define the final architecture of the ultra-lightweight hollow metallic truss cores.

Polymer templates for the core can be fabricated using various methods. We used the self-propagating photopolymer waveguide (SPPW) process for rapid, scalable, low-cost manufacturing of polymer truss structures.¹⁵ This process is fundamentally different from other additive manufacturing approaches in that it is not a layer-by-layer process; rather, the entire three-dimensional lattice architecture is formed in a single rapid exposure (30–60 s) with component area dictated solely by the size of the ultraviolet (UV) exposure source. In our SPPW process, a suitable liquid photomonomer is exposed to collimated UV light through a patterned

mask, forming an interconnected three-dimensional network of self-propagating photopolymer waveguides. A wide array of different topologies with features on the desired length scale can be manufactured by altering the incident UV exposure angle and mask pattern. Significant benefits over other additive manufacturing techniques, such as stereolithography, include improved cost, time, scalability, and surface finish.

Metal Deposition

The polymer templates were then electroless plated with approximately $0.5\ \mu\text{m}$ of nickel-phosphorus to render the surface conductive. Then, approximately $10\ \mu\text{m}$ of copper was electrolytically deposited to increase the conductivity and provide a smooth substrate for aluminum deposition and good adhesion. Nanostructured Al-Mn alloy coating was then deposited using an electrochemical plating process in a nonaqueous system.^{9,10} An electrical current was passed between two electrodes in the electrolyte to reduce the metal ions in the solution to form a solid metal coating on the truss. A periodic pulse waveform was tailored to achieve optimal deposit quality. The waveform consisted of a combination of forward and reverse current pulses on millisecond timescales. Applying pulses on this timescale allowed for selective deposition of alloying

elements and better control of the deposited structure as it grew. Due to the complex shape of the truss, nonuniform deposition was observed in areas between the struts and underneath the nodes. A simple flat anode design did not provide even current distribution into these areas, which were narrow, leading to deposits with significant thickness gradients. To address these thickness gradients, a shaped anode was specially designed to allow for better current distribution in the narrow areas of the truss. The thickness of the deposit showed improved uniformity after switching to the shaped anode (Fig. 4).

The composition of the Al-Mn alloy was tuned to achieve optimal strength and ductility properties. As the Mn content was increased, the grain size decreased, leading to increased hardness and strength (Fig. 5).

However, further increase of the Mn content eventually led to a grain structure consisting of an amorphous phase.⁹ The presence of such an amorphous phase would lead to loss of ductility (Fig. 6). Therefore, an alloy composition with between 6 at.% and 8 at.% Mn was selected to maintain a balance between strength and ductility. Figure 6 shows the results of tensile testing of subscale dog-bone samples cut from an electrodeposited coating and corresponding x-ray diffraction patterns. For comparison, a sample of aluminum alloy Al3104 was also tested. The final aluminum truss cores showed uniform thickness and consistent alloy composition with between 6 at.% and 8 at.% Mn, with hardness between 200 and 250 HV (Fig. 7). The grain size of the alloy deposited on the truss cores was approximately 20 nm, as measured by small-spot x-ray diffraction analysis and calculated using the Debye equation.

Based on Mourik et al.¹⁶ we inferred from hardness testing that the tensile strength of this alloy was approximately 750 MPa with ductility of about 10%, as indicated by the stress-strain curves in Fig. 6. The plating bath was very stable, and little variation in alloy composition or hardness was observed for over 100 A h/L (Fig. 8).

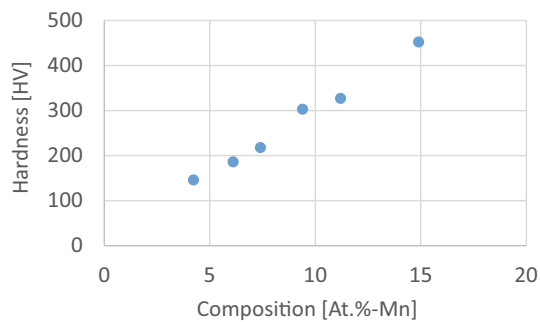


Fig. 5. Relationship between alloy composition and hardness.

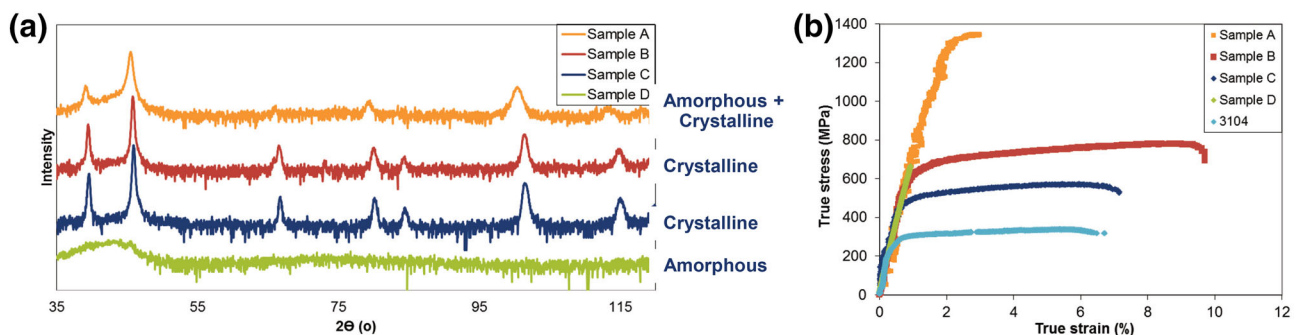


Fig. 6. (a) XRD and (b) tensile characterization showing good ductility for crystalline samples but loss of ductility upon introduction of amorphous structure.

Facesheet Integration

Two different methods were developed to attach facesheets. First, aluminum truss cores were bonded using epoxy to high-performance 8-ply IM7/8552 CFRP facesheets that were previously fabricated in a hot press (Fig. 9). The adhesive was applied locally to the nodes only, which reduces the overall amount and mass of adhesive required.

A second method to integrate truss cores with composite facesheets was developed to achieve robust mechanical attachment without adding adhesive mass while enabling facesheet fabrication directly on the core. The challenge is that the ultralightweight cores have intercell spacing and compressive strength which prevent deposition (e.g., via automatic fiber placement) or high-pressure co-curing (e.g., in an autoclave). Our approach is to use low-cost, washout casting compounds to bridge intracell volumes and provide a smooth tooling surface for high-pressure composite layup and consolidation (Fig. 10).

One of the unique attributes of a lattice design is its open cellular architecture, which allows access to the entire internal volume of the sandwich. In contrast to state-of-the-art honeycomb cores, neighboring lattice unit cells are connected in-plane via

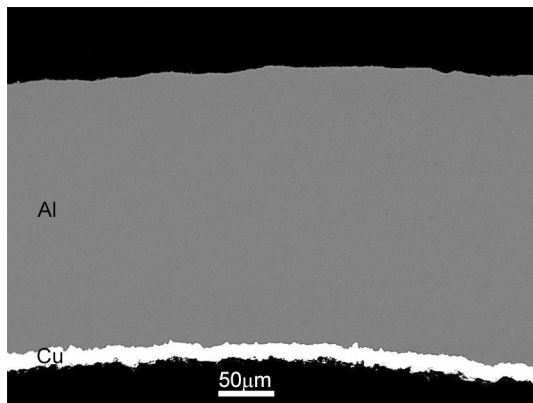


Fig. 7. Nanocrystalline Al-Mn coating with thickness of 225 μm and dense microstructure electrodeposited onto a 10- μm Cu layer.

these open pores. This connected porosity was leveraged to integrate a second, sacrificial molding material into the open volume to support the pressure applied during composite facesheet consolidation. This compaction pressure is necessary to produce facesheets with high fiber volume fraction during co-curing and is typically higher than the in-service compressive loading on an ultralight core (<2 MPa). Thus, either parasitic mass must be added to the core or the facesheets must be consolidated separately (Fig. 9), which would increase adhesive mass and manufacturing costs.

In contrast, the novel approach utilized a sacrificial mold for in-series load bearing during consolidation (Fig. 10). An initially liquid mold material was injected into the open volume of the core, then allowed to solidify in net shape around the lattice. The interface between the facesheets and the core was controlled by means of interposer layers, which allowed for projection of the lattice nodes above the surface of the mold. For this study, a commercially available washout ceramic mandrel material (Aquadour, ACM) was chosen for the sacrificial mold.¹⁷ An additional 10% by weight of water-soluble polymer binder was added to the Aquadour material to ensure consistent filling around lattice members of different geometries.

After infiltration and firing of the ceramic mold, unidirectional IM7/8552 composite facesheets were laid up and consolidated directly on the mold/lattice surface under representative autoclave conditions (0.7 MPa, 177°C for 6-h cycle). The ceramic mold was then removed from the lattice core interior by rinsing with 40°C water. This resulted in a direct bond between the composite facesheets and the lattice core, although the 1.6-mm-thick interposer layer proved to be too large, leading to deflection of the composite facesheets in the region around the lattice nodes (Fig. 11d).

Mechanical Testing

Shear testing was performed according to ASTM C273. Core samples with dimensions of $55 \times 160 \times 25.4$ mm³ comprising five unit cells

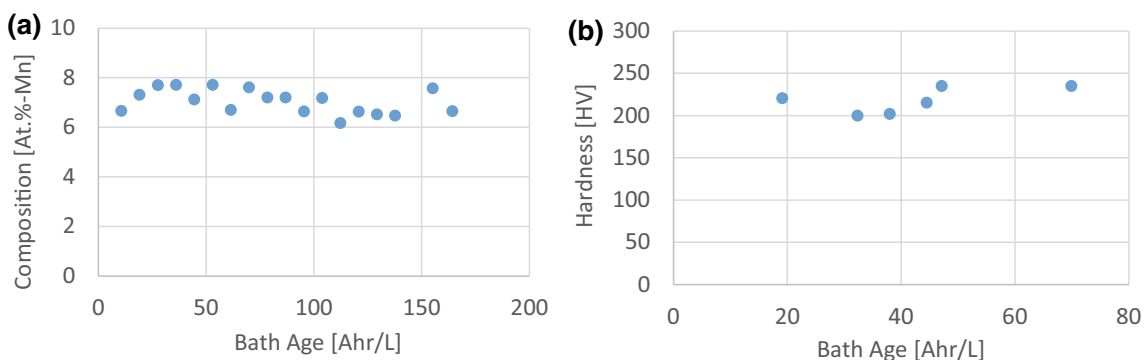


Fig. 8. (a) Alloy composition and (b) hardness as function of plating bath age.

were bonded to steel plates by applying 3M[®] DP460NS adhesive to the nodes only using a glue gun. The cores were tested in single-lap configuration with displacement control at 1 mm/min (Fig. 12). The failure mode is brittle fracture in tension, as evidenced by the formation of large cracks in the struts that are loaded in tension (Fig. 12a). Typically, one crack forms first, causing a drop in strength, then after additional loading, more cracks form on other tensile load-bearing struts, leading to the stress–strain curve shown in Fig. 12b. It is believed that porosity in the aluminum deposit as well as surface roughness initiated cracks. These defects lead to lower strength than predicted by finite element simulation and large scatter in the data. However, the samples with the highest-quality plating showed $2 \times$ higher shear strength than high-performance aluminum 5056 honeycomb cores. Figure 12d summarizes the shear test results. The shear strength was measured on single samples of the truss core, but since the truss cores were designed to be interlaced for the intended application, the measured density and strength values were also doubled and presented with hollow markers. The results are compared with the shear strength value of aluminum alloy Al 5056

honeycomb cores in the strong direction (L direction), provided by the manufacturer, Hexcel Corp.¹⁸ The tabulated strength of these aerospace-grade, high-strength honeycomb cores was scaled to 25.4 mm core thickness using the equation provided by Hexcel.¹⁹ Data for closed-cell polyvinyl chloride (PVC) polymer foams (Divinycell[®] H)²⁰ are also shown, representing an alternative core material for lightweight sandwich structures.

Compression testing was performed on single unit cells bonded to aluminum facesheets to obtain a maximum number of data points (Fig. 13). Failure occurred by brittle fracture in the region beneath the top node, where the tensile stress induced by strut bending is the highest. Since axial compression mitigates some of the bending-induced tensile stress, brittle fracture is delayed to higher macroscopic loads when the core is loaded in compression. Accordingly, the stress–strain curve shows some yielding followed by failure and termination of the test. Test results are summarized in Fig. 13c. Similar to the shear results, a relatively large variation in strength is measured, presumably due to large flaw populations and nonuniformities in the samples, which were fabricated in different batches over 6 months. A $2\text{--}4\times$ increase in compression strength over aerospace-grade Al 5056 honeycomb cores is seen for the samples with the highest measured compressive strengths.

To test the performance of truss core sandwich panels with CFRP facesheets, four-point bending and edgewise compression tests (ASTM C393 and C364) were performed in direct comparison with honeycomb core panels. Four-point bending testing showed failure of the core for both truss and honeycomb as expected. Edgewise compression testing showed adhesive failure in the truss core panel once the facesheets buckled. The honeycomb panel



Fig. 9. Sandwich panels ($30 \times 30 \times 3 \text{ cm}^3$) with nanocrystalline Al-Mn truss core and CFRP facesheets fabricated for testing.

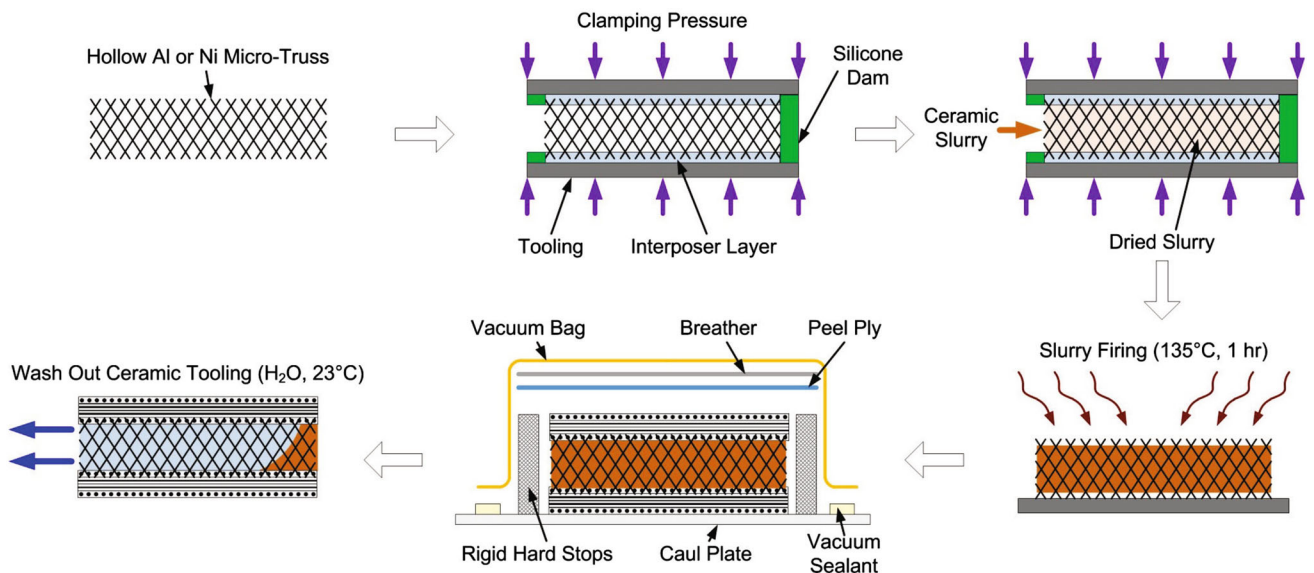


Fig. 10. Schematic approach for facesheet co-curing directly on the core.

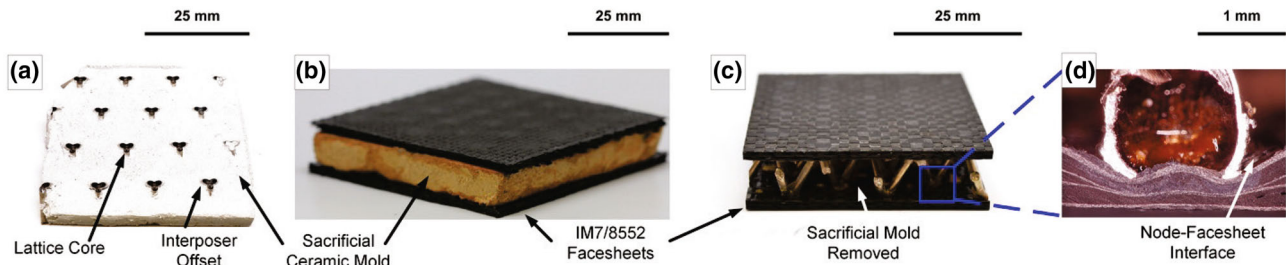


Fig. 11. Demonstration of facesheet integration by co-curing: (a) sacrificial mold integrated in lattice core, (b) facesheet consolidation on mold/lattice, (c) mold removal, and (d) lattice core/facesheet interface.

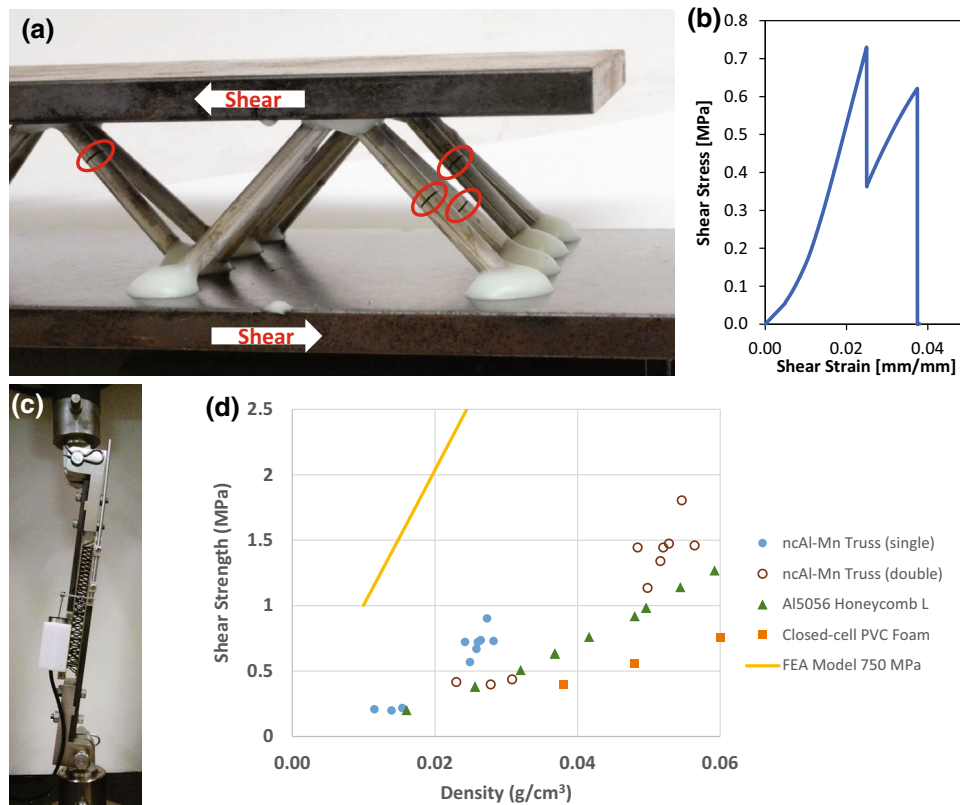


Fig. 12. Results of shear testing of nanocrystalline Al-Mn truss cores: (a) typical failure mode and (b) stress–strain curve, (c) shear test setup, and (d) comparison of results with state of the art and simulation.

failed in the core by tension. The core–facesheet interface limited the strength of the truss core sandwich panel in edgewise compression, which could be overcome by choosing a stronger adhesive or increasing the interface area. A sandwich core with lower thickness H would allow for more nodes in contact with the facesheets for given area.

DISCUSSION

While nanocrystalline aluminum-manganese truss cores surpass the strongest commercially available aluminum honeycombs, simulations predict that even higher strength could be achieved. The discrepancy between the simulated and measured strength is due to porosity, surface roughness,

and nonuniform thickness distribution. Additional process development is required to mitigate these issues, especially in such thick (200–300 μm) electrodeposited material. Cores with lower density and thickness H would require thinner aluminum deposits, facilitating reductions in porosity, surface roughness, and nonuniformity.

One advantage of the truss cores presented herein is the ability for net-shape fabrication. The core templates can be shaped easily in the polymer state, before depositing the metal. Figure 14a shows a highly curved sandwich panel with a truss core that was fabricated by heating the polymer template above its glass-transition temperature, bending it to the required shape in a mandrel, cooling it down to

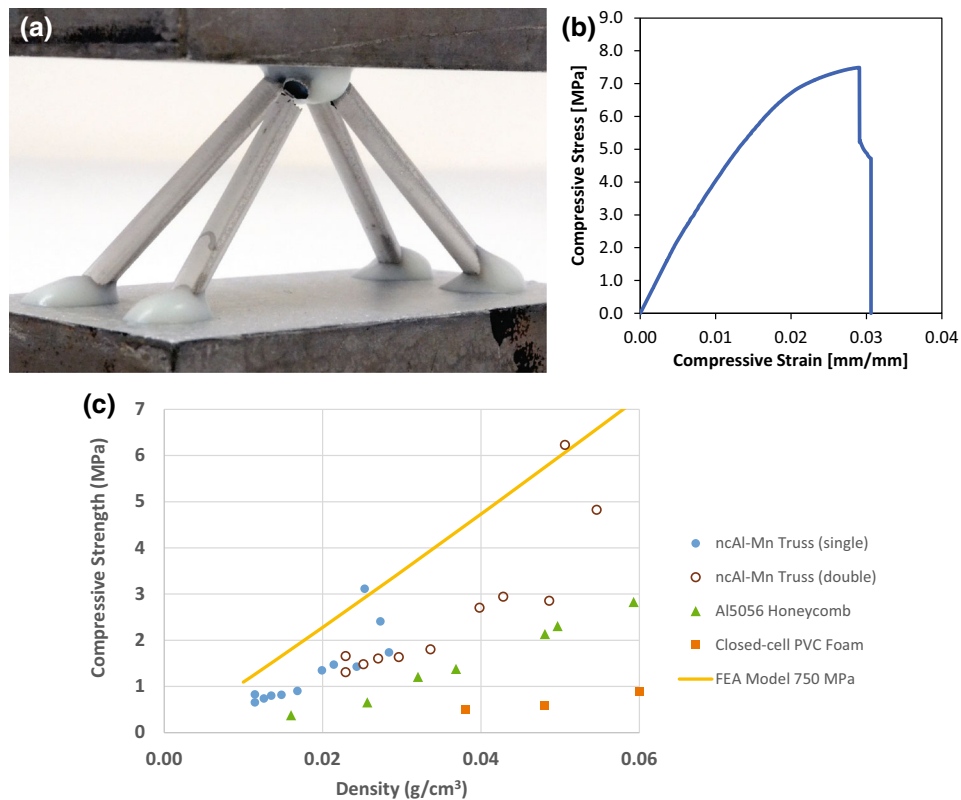


Fig. 13. Results of compression testing of nanocrystalline Al-Mn truss cores: (a) typical failure mode and (b) stress–strain curve, (c) comparison of results with state of the art and simulation.

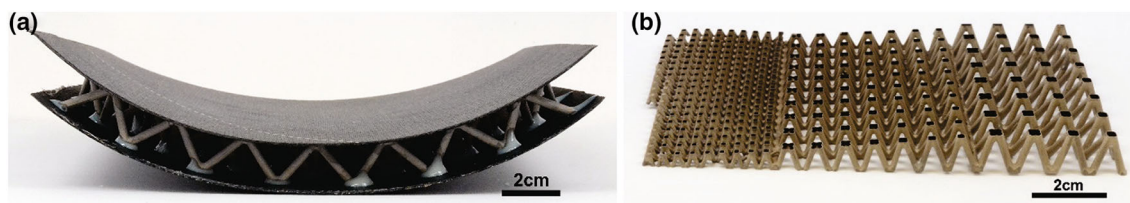


Fig. 14. Net-shape cores with (a) high curvature and (b) graded architecture enabled by the templating approach.

lock in that shape, and subsequently electroplating it. Furthermore, polymer core templates with complex shapes and graded architectures can be additively manufactured, as shown in Fig. 14b. Hexagonal honeycomb is difficult to fit into curved structures due to its anticlastic curvature behavior and must be machined to the required shape from expanded blocks, adding manufacturing cost.

Galvanic corrosion has been an issue for sandwich panels with aluminum cores and CFRP facesheets due to their different electrochemical potential, especially in applications where moisture is present and long life is required. A thin layer of insulating glass scrim can be inserted between the core and the facesheet to block the electrochemical reaction and mitigate galvanic corrosion. Alternatively, a thin coating of a metal with higher potential such as

copper or nickel can be electrodeposited on the surface of the aluminum truss to protect it from galvanic corrosion.

Over recent years, several new microarchitected cellular materials have been developed. While nanolattices²¹ and nano-honeycombs²² can take advantage of strengthening effects from nanoscale phenomena, it is not envisaged that fabrication of these materials at scales above 1 mm³ will be possible in the near future, and they are not therefore industrially relevant. Microlattices with multiple layers of unit cells cannot achieve the compressive strength of conventional aluminum honeycomb^{7,23} because of premature failure at the nodes. This is due to nodal rotation and stress concentration. The only other core materials that could surpass aluminum honeycombs are CFRP-

based honeycombs or truss cores currently under development.²⁴ However, composite processing adds a different set of challenges.

CONCLUSION

An approach to manufacture lightweight sandwich structures with high-strength, nanocrystalline aluminum truss cores has been demonstrated. By electrodepositing nanocrystalline aluminum-manganese alloy onto polymer templates, this extraordinary thin-film material can be converted into a three-dimensional hollow truss structure. Film thicknesses of 300 μm and more were achieved, and the scalability of the process was demonstrated by fabricating 30 cm \times 30 cm \times 3 cm sandwich panels. Mechanical testing was conducted in compression and shear, and improvements of 2–4 times over state-of-the-art aluminum honeycombs was realized. Simulations predict that further improvements are possible if the plating uniformity can be increased and the porosity and surface roughness decreased. While this study focused on large, flat sandwich panels with 3 cm thickness, this technology appears more advantageous for curved, net-shaped structures with thinner cores. The open-celled nature of the truss cores enables novel strategies for facesheet integration, such as co-curing, which eliminates the need for extra adhesive.

ACKNOWLEDGEMENTS

This work was supported by NASA's Space Technology Mission Directorate under the Game Changing Development Program through Contract No. NNC15CA16C. The authors thank Shiyun Ruan (Xtallic) for useful discussions.

REFERENCES

1. L.J. Gibson, M.F. Ashby, *Cellular Solids: Structure and Properties* (Cambridge: Cambridge University Press, 1999).
2. D.J. Sypeck and H.N.G. Wadley, *Adv. Eng. Mater.* 4, 759 (2002).
3. H.N.G. Wadley, N.A. Fleck, and A.G. Evans, *Compos. Sci. Technol.* 63, 2331 (2003).
4. E.C. Clough, J. Ensberg, Z.C. Eckel, C.J. Ro, and T.A. Schaedler, *Int. J. Solids Struct.* 91, 115 (2016).
5. D.T. Queheillalt and H.N.G. Wadley, *Acta Mater.* 54, 303 (2005).
6. D.T. Queheillalt and H.N.G. Wadley, *Int. J. Solids Struct.* 102, 389 (2011).
7. T.A. Schaedler, A.J. Jacobsen, A. Torrents, A.E. Sorensen, J. Lian, J.R. Greer, L. Valdevit, and W.B. Carter, *Science* 334, 961 (2011).
8. K.J. Maloney, C.S. Roper, A.J. Jacobsen, W.B. Carter, L. Valdevit, and T.A. Schaedler, *APL Mater.* 1, 022106 (2013).
9. S.Y. Ruan and C.A. Schuh, *J. Mater. Res.* 27, 1638 (2012).
10. S.Y. Ruan and C.A. Schuh, *Acta Mater.* 57, 3810 (2009).
11. R.D. Hilty, L. J. Masur, *JOM* (2017). doi:10.1007/s11837-017-2499-z.
12. Granta Design Limited, *CES Selector* software and database (2013).
13. M.F. Ashby, *Materials Selection in Mechanical Design* (Oxford: Butterworth-Heinemann, 2011).
14. L. Valdevit, S.W. Godfrey, T.A. Schaedler, A.J. Jacobsen, and W.B. Carter, *J. Mater. Res.* 28, 2461 (2013).
15. A.J. Jacobsen, W.B. Carter, and S. Nutt, *Adv. Mater.* 19, 3892 (2007).
16. P. van Mourik, J. van Dam, and S. Picken, *Materials Science in Design and Engineering* (Delft: VSSD, 2012).
17. R. Vaidyanathan, J. Campbell, G. Artz, S. Yarlagadda, J.W. Gillespie, D. Dunaj, B. Guest, K.L. Nesmith, A water soluble tooling material for complex polymer composite components, in *SAMPE Conference Proceedings* (2003).
18. Hexcel Corporation, Stamford Connecticut, HexWeb[®] CR III Data Sheet (2015). http://www.hexcel.com/Resources/DataSheets/Honeycomb-Data-Sheets/CR3_us.pdf.
19. Hexcel Corporation, HexWeb[™] Honeycomb Attributes and Properties (1999). http://www.hexcel.com/Resources/DataSheets/Brochure-Data-Sheets/Honeycomb_Attributes_and_Properties.pdf.
20. Diab Group, Laholm Sweden, Divinycell H Data Sheet (2016). <http://www.diabgroup.com/en-GB/Products-and-services/Core-Material/Divinycell-H>.
21. L.R. Meza, S. Das, and J.R. Greer, *Science* 345, 1322 (2014).
22. J. Bauer, S. Hengsbach, I. Tesari, R. Schwaiger, and O. Kraft, *PNAS* 111, 2453 (2014).
23. X. Zheng, H. Lee, T.H. Weisgraber, M. Shusteff, J. DeOtte, E.B. Duoss, J.D. Kuntz, M.M. Biener, Q. Ge, J.A. Jackson, S.O. Kucheyev, N.X. Fang, and C.M. Spadaccini, *Science* 344, 1373 (2014).
24. K. Finnegan, G. Kooistra, H.N.G. Wadley, and V.S. Deshpande, *Int. J. Mater. Res.* 98, 1264 (2007).